Electronic Supplementary Information

Self-templated fabrication of $FeMnO_3$ nanoparticle-filled polypyrrole nanotubes for peroxidase mimicking with a synergistic effect and their sensitive colorimetric detection of glutathione

Maoqiang Chi, Sihui Chen, Mengxiao Zhong, Ce Wang, Xiaofeng Lu*

Alan G. MacDiarmid Institute, College of Chemistry, Jilin University, Changchun, 130012, P. R. China.

*Corresponding author

Email: xflu@jlu.edu.cn

Tel: +86 431 85168292

Fax: +86 431 85168292

Experimental section

Materials

Polyvinyl pyrrolidone (PVP, M_w=1300000 g mol^{-1}) was purchased from Sigma-Aldrich. Manganese(II) acetate tetrahydrate ($Mn(Ac)_2 \cdot 4H_2O$) and iron(III) nitrate nonahydrate ($Fe(NO_3)_3 \cdot 9H_2O$) were obtained from Huadong Chemical Industry (Tianjin) Co., Ltd and Tianjin Guangfu Fine Chemical Research Institute, respectively. 3,3',5,5'-tetramethylbenzidine (TMB) was purchased from Sinopharm chemical reagent Beijing Co., Ltd. Pyrrole and dimethyl sulfoxide (DMSO) were provided by Aladdin. N,N-dimethylformamide (DMF) was bought from Tiantai Fine Chemical Co., Ltd. Hydrochloric acid (HCl), H_2O_2 and ethanol were obtained from Beijing Chemical Works. All the chemicals mentioned in this work were used as received without any further purification.

Fabrication of $FeMnO_3$ nanofibers via an electrospinning and calcination process

$FeMnO_3$ nanofibers were prepared by a typical electrospinning technique and calcination process. Firstly, 0.245 g of $Mn(Ac)_2 \cdot 4H_2O$ and 0.404 g of $Fe(NO_3)_3 \cdot 9H_2O$ were dissolved in a mixed solvent consisting of 3 mL of ethanol and 3 mL of DMF under vigorous stirring for 1 h, then 0.47 g of PVP was slowly added. After constant stirring for 12 h, a homogeneous viscous solution was obtained. Secondly, the as prepared solution was electrospun using a glass syringe with a tip inner at an applied voltage of 15 kV over a distance of 20 cm between the syringe tip and the aluminum foil collector. Finally, the PVP/$Fe(NO_3)_3$/$Mn(Ac)_2$ fibrous membranes were prepared on the aluminum foil. To prepare $FeMnO_3$ nanofibers, the electrospun PVP/$Fe(NO_3)_3$/$Mn(Ac)_2$ fibrous membrane was peeled off from the collector and was calcined at 550 °C in air for 3 h referring to a defined heating program. Then, a rufous colored powder of the $FeMnO_3$ nanofibers was obtained.

Fabrication of $FeMnO_3$ nanoparticle-filled polypyrrole nanotubes

A total of 5 mg $FeMnO_3$ nanofibers were put into a small beaker and then transferred into a vacuum desiccator equipped with 0.3 mL of pyrrole and 2.4 mL of

HCl (5 M) in two separated small bottles. After evacuation for about 5 min, the vacuum desiccator was left at room temperature for 0.5 h, 1 h, 2 h, and 3 h, respectively, to fabricated $FeMnO_3$ nanoparticle-filled PPy nanotubes ($FeMnO_3$@PPy nanotubes) with different PPy shell thickness.

Peroxidase-like catalytic activities of $FeMnO_3$@PPy nanotubes

To evaluate the peroxidase-like activity of $FeMnO_3$@PPy nanotubes, a colorimetric experiment toward the oxidation of TMB substrate in the presence of H_2O_2 was applied. In a typical procedure, 20 μL of TMB solution (15 mM in DMSO) and 20 μL of H_2O_2 (30 wt%) were added into 3 ml of acetate buffer solution (pH = 4.0, unless otherwise stated). After that, 20 μL of $FeMnO_3$ nanofibers and $FeMnO_3$@PPy nanotubes aqueous suspension (3.0 mg ml^{-1}) was injected into the solution mentioned above. Catalytic activity measurements were conducted by monitoring the absorbance changes at 651 nm in time course mode. The steady-state kinetics analysis was carried out by keeping the concentration of H_2O_2 constant and varying the concentrations of TMB when using TMB as substrate. On the contrary, the concentration of TMB was fixed and the concentration of H_2O_2 was changed for H_2O_2 as substrate.

Colorimetric detection of H_2O_2 and glutathione (GSH)

For the colorimetric detection of H_2O_2, varied concentrations of H_2O_2, together with 20 μL of TMB (15 mM) and 20 μL of catalyst (3 mg mL^{-1}) was added into 3 mL of acetate buffer solution (pH = 4.0). Then time-course detection with UV-vis spectrometer at 651 nm for 600 s was applied to achieve a dose of H_2O_2 concentration-dependent responsive curves. The colorimetric detection of GSH is similar with the detection of H_2O_2. In a typical procedure, varied concentrations of GSH was added into 3.0 mL of acetate buffer solution (pH = 4) containing 20 μL of catalyst suspension (3 mg mL^{-1}), 20 μL of TMB solution (15 mM DMSO) and 20 μL of H_2O_2 (30 wt%). Then UV-vis absorbance spectroscopy at 651 nm was used to monitor the absorbance changes. To elevate the selectivity of the proposed detection method, 80 μM of phenylalanine (Phe), histidine (His), tryptophan(Trp), methionine (Met), tyrosine (Tyr), valine (Val), uric acid (UA), lysine (Lys), L-cysteine (Cys),

homocysteine (Hcy), glucose (Glu), NaCl, KCl, $CaCl_2$ were added into the above reaction system instead of GSH.

Analysis of GSH in human serum samples

Human serum samples were donated by Changchun Sino-Japanese Friendship Hospital (Changchun, China). For the colorimetric detection of GSH in human serum samples, 20 μL of TMB solution (15 mM in DMSO) and 20 μL of H_2O_2 (30 wt%) were added into 3 mL of acetate buffer solution (pH = 4.0) containing 20 μL of human serum samples. After that, 20 μL of catalyst aqueous suspension (3.0 mg ml^{-1}) was injected into the solution mentioned above. Then UV-vis absorbance spectroscopy at 651 nm was used to monitor the absorbance changes for 600 s, the maximum absorbance was collected for analysis. After that, different concentrations (4 μM, 6 μM and 8 μM) of GSH were added for spiking. The concentration of GSH in the serum samples was quantified by the linear equation.

Characterization

The morphologies of the as-prepared samples were characterized by field emission scanning electron microscopy (SEM, FEI Nova NanoSEM 450) and transmission electron microscopy (TEM, JEOLJEM-1200 EX) operated at 15 and 100 kV, respectively. High-resolution transmission electron microscopy (HRTEM) images with selected area electron diffraction (SAED) patterns and energy dispersive X-ray (EDX) analysis were obtained using a FEI Tecnai G2 F20 high resolution transmission electron microscope operated at a 200 kV accelerating voltage. X-ray diffraction (XRD) patterns were obtained with an x-ray diffractometer (Empyrean, PANalytical B.V.) based on Cu-Ka radiation in the range of 10-90°. Analysis of the X-ray photoelectron spectra (XPS) was performed on a Thermo ESCALAB 250 spectrometer. Fourier transform infrared (FTIR) spectroscopy was used to record FTIR spectra by BRUKER VECTOR 22 Spectrometer using KBr powder-pressed pellets. UV–vis absorption spectroscopy was performed on a Shimadzu UV-2501 PC spectrometer.

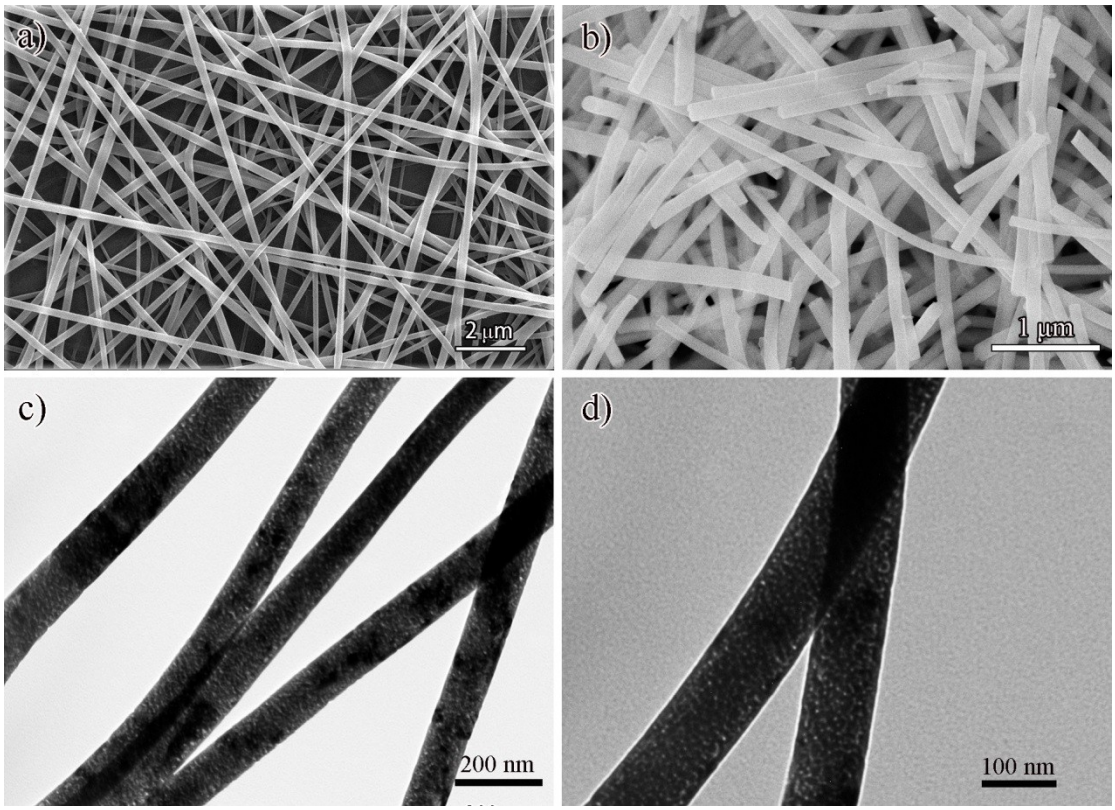

Figure S1. a) SEM image of the electrospun PVP/$Fe(NO_3)_3$/$Mn(Ac)_2$ nanofibers; b) SEM image of the calcined $FeMnO_3$ nanofibers; c, d) TEM images of the prepared $FeMnO_3$ nanofibers with a low and high magnifications.

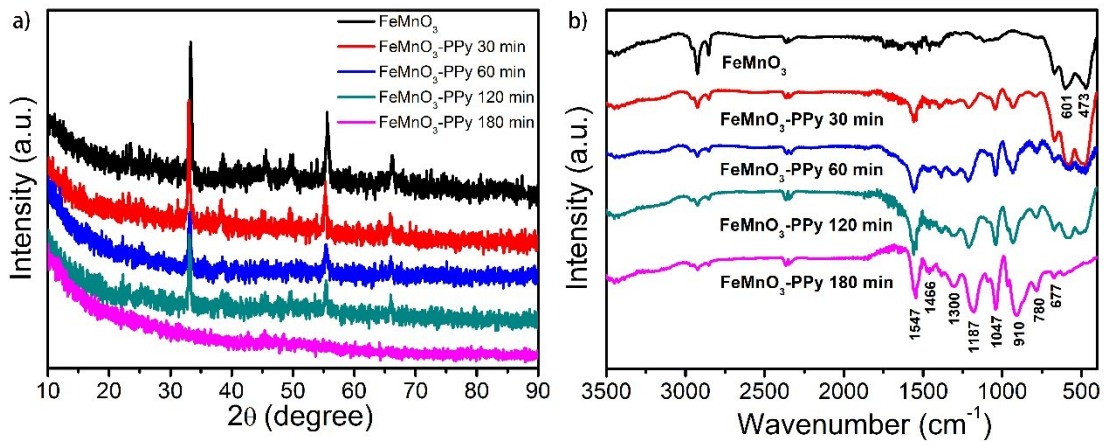

Figure S2. a) XRD patterns and b) FTIR spectra of $FeMnO_3$ nanofibers and $FeMnO_3$@PPy nanotubes with different polymerization time of 30, 60, 120 and 180 min, respectively.

As shown in Figure S2a, the XRD diffraction peaks centered at around 2θ =23.3°, 33.1°, 38.6°, 45.3°, 49.6°, 55.5° and 66.1° are attributed to (211), (222), (400), (332), (134), (440) and (622) planes of the crystallographic cubic perovskite structure of $FeMnO_3$ (JCPDS 76-0076).[1] The Fourier-transform infrared (FTIR) spectrum of the $FeMnO_3$ nanofibers is supplemented in Figure S2b. It is clearly observed that the absorption peaks at 473 and 601cm^{-1} are assigned to Mn-O and Fe-O vibrations, respectively.[2]

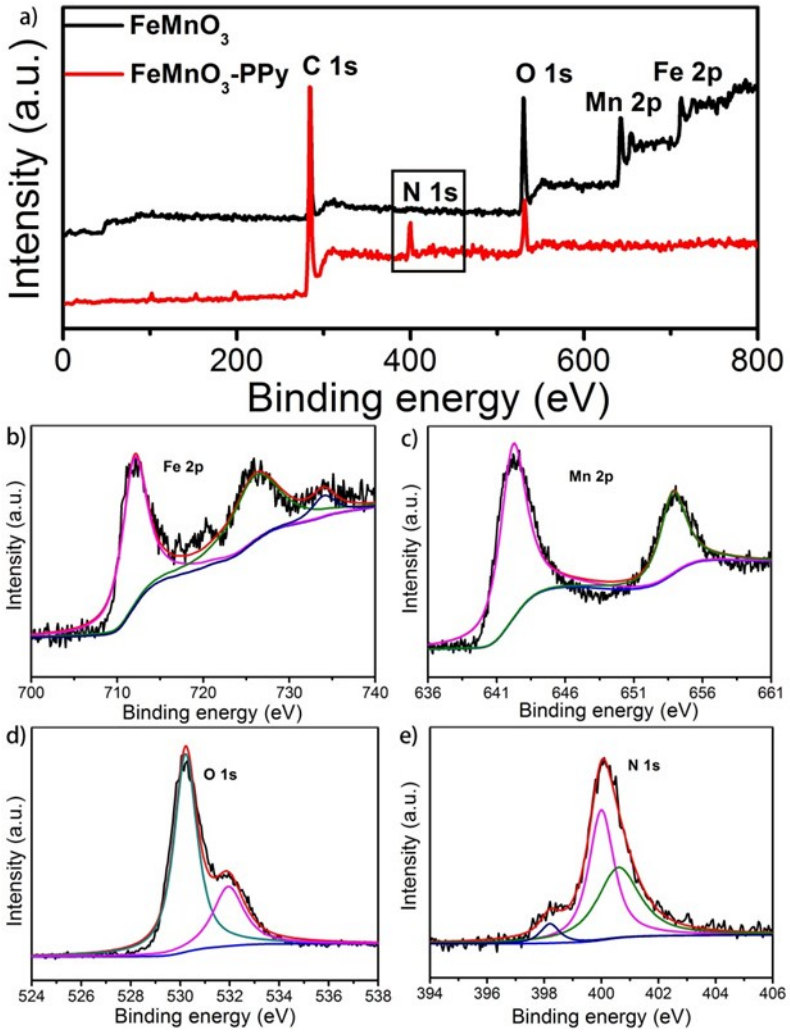

Figure S3. XPS spectra of the as-prepared $FeMnO_3$ nanofibers and $FeMnO_3$@PPy nanotubes: a) full survey spectrum, b) Fe 2p, c) Mn 2p and d) O 1s region in XPS spectrum of $FeMnO_3$ nanofibers, e) N 1s region in XPS spectrum of $FeMnO_3$@PPy nanotubes.

The chemical composition and oxidation state of the $FeMnO_3$ nanofibers are further investigated by X-ray photoelectron spectroscopy (XPS). As displayed in Figure S4a, the wide-scan XPS spectrum evidently exhibits the signals of Fe, Mn and O elements in $FeMnO_3$ nanofibers. In detail, two peaks located at 712.1 and 726.5 eV with a satellite peak at 734.2 eV can be indexed to Fe^{2+} (Figure S4b). Two characteristic peaks of Mn 2p located at 642.2 eV (Mn $2p_{3/2}$) and 653.9 eV (Mn $2p_{1/2}$) are attributed to Mn^{4+} with no signal of other valence states of the manganese ions (Figure S4c). In O1s spectrum, the peak at around 530.2 eV is ascribed to the lattice oxygen in Fe/Mn-O framework, while another at around 531.9 eV is related to the hydroxyl group (Figure S4d).[1,3]

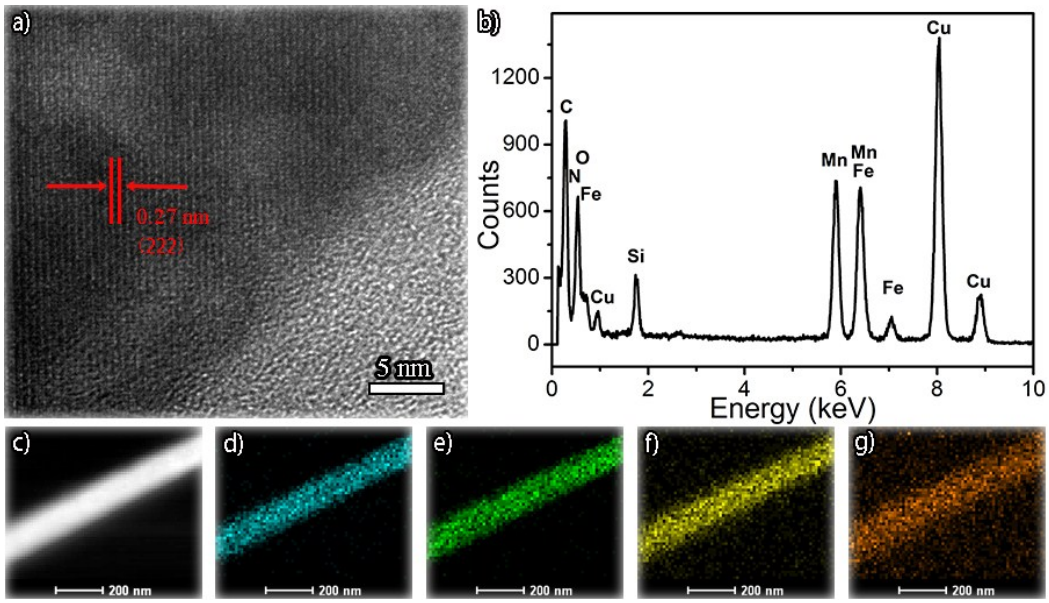

Figure S4. a) HRTEM image and b) EDX spectrum of the prepared $FeMnO_3$@PPy nanotubes; c) HAADF-STEM pattern and EDX element mapping images of d) Fe-K, e) Mn-K, f) O-K, g) N-K in $FeMnO_3$@PPy nanotubes.

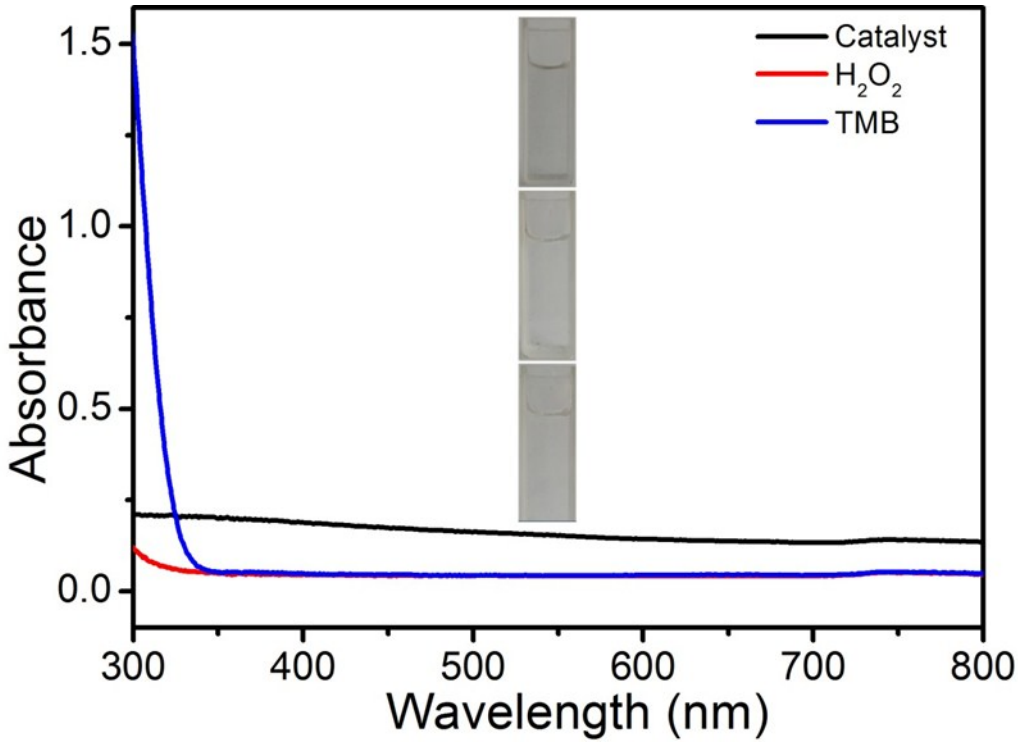

Figure S5. UV-vis absorbance curves of absorption mode against catalyst, TMB and H_2O_2 at 10 min in acetate buffer solution (pH = 4), the inset displays the pertinent photographs.

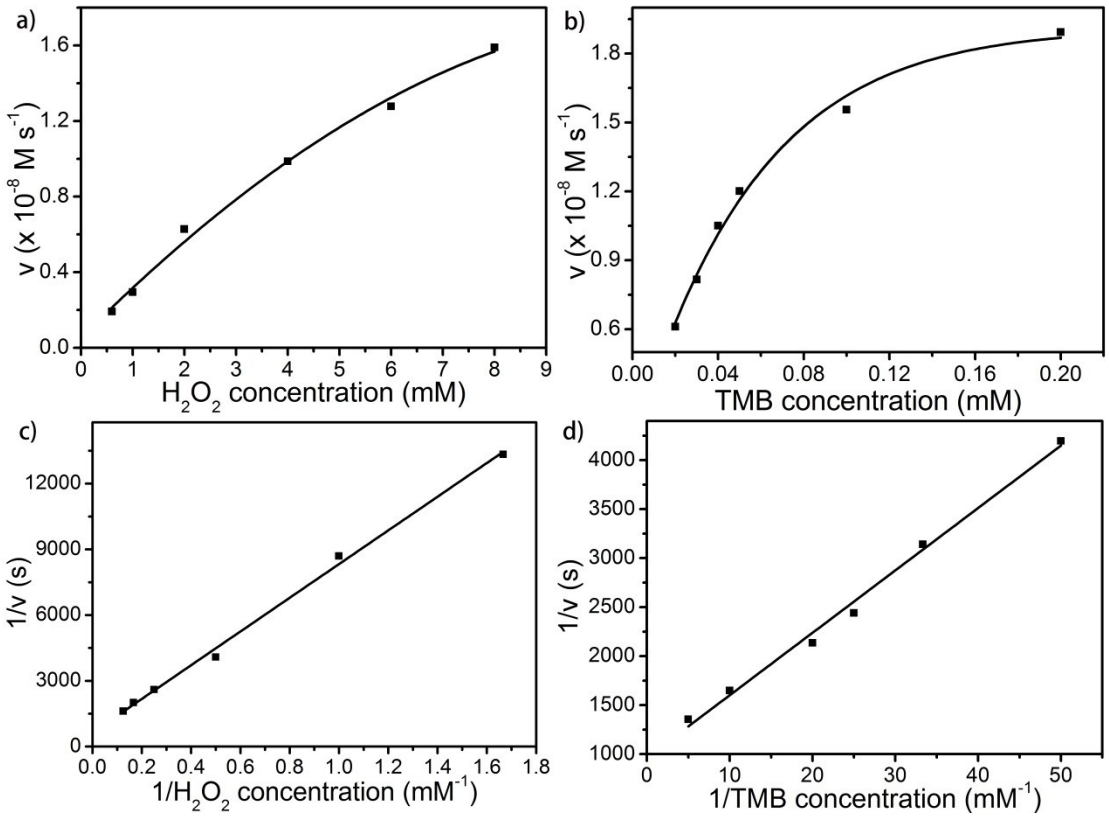

Figure S6. Steady-state kinetic experiments of $FeMnO_3$@PPy nanotubes. The catalyst concentration was kept constant at 20 μg mL^{-1} in 3 mL of acetate buffer solution (pH = 4). a) The concentration of TMB was fixed at 100 μM and the H_2O_2 content was varied; b) H_2O_2 concentration was maintained at 5 mM with various concentrations of TMB; c, d) The corresponding double reciprocal plots of H_2O_2 and TMB.

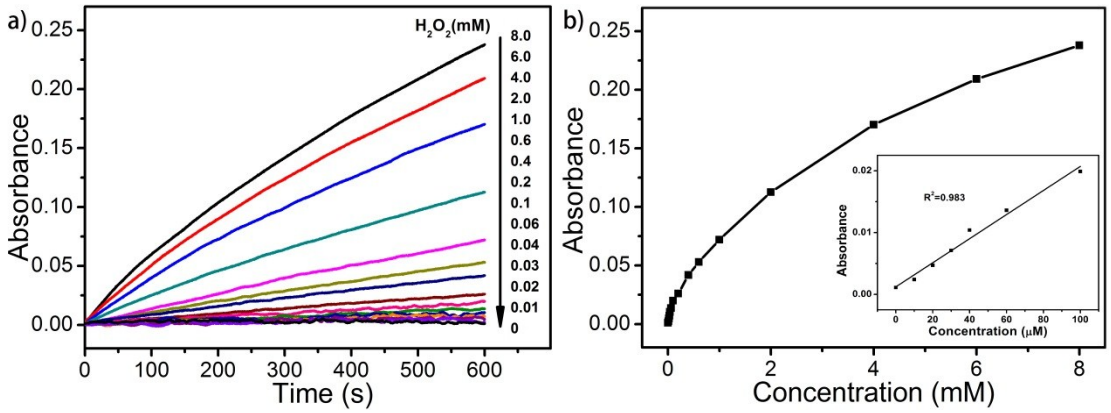

Figure S7. a) The absorbance changes of the catalytic oxidation of TMB by the as-prepared $FeMnO_3$@PPy nanotubes in the absence or presence of H_2O_2 with various concentrations under an optimal acetate buffer solution (pH = 4); b) The dose–response curve with regard to the detection of H_2O_2, and the inset photograph exhibits the corresponding calibration line.

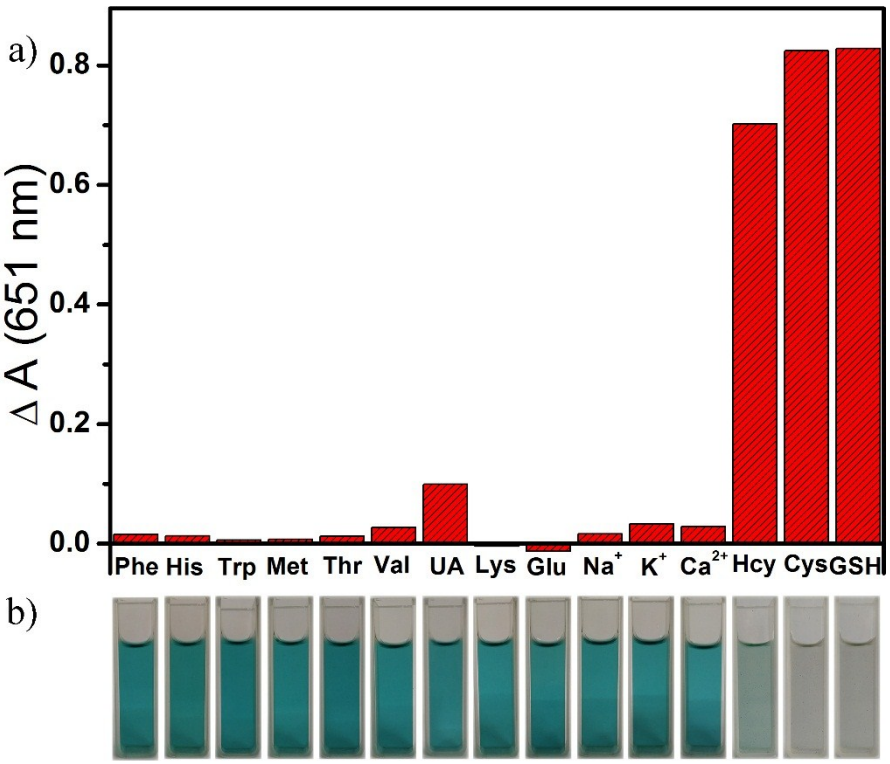

Figure S8. a) The difference values of absorbance at 651 nm between 0 min and 10 min in diverse systems containing fixed concentrations of TMB (0.1 mM), H_2O_2 (65 mM), catalyst solution (20 μg mL^{-1}) with GSH (80 μM) or other different interferential substances (80 μM); b) The corresponding photographs of the above reaction solutions on 10 min.

Table 1. Comparison of the LOD values among the detection system in this work and the previous reported enzyme-like colorimetric detection approaches.

Nanomaterials	Linear range (μM)	LOD (μM)	References
Fe_3O_4 MNPs	3-30	3	[12a]
CBT-Cys(SEt)	0-87	11	[12b]
BSA-MnO_2 NPs	0.26-26	0.1	[12c]
C-dot-Ni(IV)	312-31200	203	[12d]
Ag^+	0.05-8	0.05	[12e]
$Cu_{1.8}S$ NPs	500-10000	60	[12f]
MOFs	0.075-0.475	0.125	[12g]
AuNCs	2-25	0.42	[12h]
MnO_2 nanosheets	0-150	0.38	[12i]
ABTS-Ag^+	0.1-4	0.059	[12j]
$FeMnO_3$@PPy	0-10	0.036	This work

Table 2. Determination of GSH concentration in serum samples.

Serum sample (150-folds diluted)	Without spiking (μM) ± SD (n=3)	GSH spiking (μM)	GSH measured (μM) ±SD (n=3)	Recovery(%)
Sample 1	6.108 ± 0.092	4	10.116 ± 0.454	100.2
Sample 2	6.450 ± 0.207	6	12.727 ± 0.533	104.6
Sample 3	6.148 ± 0.403	8	14.412 ± 0.260	103.3

References

1. M. Li, W. Xu, W. Wang, Y. Liu, B. Cui and X. Guo, *J. Power Sources*, 2014, **248**, 465-473.
2. M. H. Habibi and V. Mosavi, *J. Mater. Sci.: Mater. Electron.*, 2017, **28**, 8473-8479.
3. Z. Yang, F. Ma, Y. Zhu, S. Chen, C. Wang and X. Lu, *Dalton Trans*, 2017, **46**, 11171-11179.